# Supporting Information

Qiu et al. 10.1073/pnas.1714421115

## SI Materials and Methods

**Characterization.** TEM and HR-TEM were employed to characterize the morphology and elemental composition of BPNSs, and SAED and energy-dispersive X-ray spectrometry (EDS) were operated at 300 kV by using the FEI Tecnai $G^2$ F30 field-emission TEM equipment. AFM was employed to characterize the morphology and height of BPNSs by using an ICON Bruker system in tapping mode, with the samples dispersed on $Si/SiO_2$ substrates by a drop-casting method and the images (512 pixels per line) recorded at a scan rate of 1.79 Hz. XPS was performed to analyze the surface chemicals of BPNSs on the ULVAC PHI 5000 Versa Probe II, using an Al $K_\alpha$ ($\lambda$ = 0.83 nm, h$\upsilon$ = 1486.7 eV) X-ray source operated at 23.5 W, and the data were analyzed by the MultiPak Version 9.0 software. The Raman spectrum was acquired by the Reishawin Via confocal Raman microscope equipped with a 514-nm Argon ion laser as the excitation source. Fourier transform infrared spectrophotometer (FTIR) spectra were used to confirm the BPNSs and PEGylated BPNSs. UV-Vis spectroscopy was performed by the Perkin-Elmer LAMBDA 750 Spectrophotometer to measure the optical absorbance of BP in the range of 200–1,100 nm, using prealigned tungsten–halogen and deuterium lamps as the incident light source.

**Cell Culture Assays.** MDA-MB-231 (human breast cancer cells), A549 (A549 human lung carcinoma cells), HeLa (human cervical cancer cell), and B16 (mouse melanoma cells) were from American Type Culture Collection (ATCC). MDA-MB-231, A549, HeLa, and B16 cells were cultured in normal RPMI-1640 medium with 10% FBS and 1% penicillin/streptomycin at 37 °C with 5% $CO_2$.

**In Vitro Toxicity and Safety Study.** MDA-MB-231, A549, HeLa, and B16 cells were seeded at a density of 8,000 cells per well in 96-well plates and incubated overnight. Afterward, the cells were incubated with BPNSs at different BP concentrations (1 μg/mL, 50 μg/mL, 100 μg/mL, and 200 μg/mL) for 48 h (fresh media with the same BP concentrations were changed every day). Five multiple holes were set for every sample. The culture medium was replaced with CCK-8 reagent, and an additional 1-h incubation was conducted for the cells at a determined time. Then a microplate reader (ELx808; BioTek) was used to measure the absorbance at 450 nm. Untreated cells were represented as control group.

**Annexin V-FITC/PI Double-Staining Assay.** MDA-MB-231cells were incubated with BP@Hydrogels and irradiated with an 808-nm laser at a power density of 1 W/$cm^2$ for different times (0 min, 5 min, 10 min, 15 min). After incubation for another 12 h, MDA-MB-231 cells were harvested, washed, and resuspended with PBS. Apoptotic cells were determined with a TransDetect Annexin V-FITC/PI Cell Apoptosis Detection Kit (Transgen Biotech) according to the manufacturer's protocol. Briefly, the cells were washed and subsequently incubated for 15 min at room temperature in the dark in 100 μL of 1× binding buffer containing 5 μL of PI and 5 μL of Annexin V-FITC. Afterward, apoptosis was analyzed by a DxFLEX Flow Cytometer (Beckman Coulter).

**In Vivo Anticancer Therapy.** Female BALB/c (nu/nu) mice (5 wk old) were purchased from Guangdong Medical Laboratory Animal Center. The tumor model was generated by injecting MDA-MB-231 cells ($5 \times 10^6$ per mouse) into the left axilla of each mouse. When the tumor volumes reached about 100 $mm^3$, tumor-bearing mice were randomly divided into four groups (five mice for each group). Groups 1–4 were intratumorly injected with 100 μL saline, 200 μg/mL DOX, BP@Hydrogel (500 μg/mL BP, 200 μg/mL DOX, 1% LA), and BP@Hydrogel (500 μg/mL BP, 200 μg/mL DOX, 1% LA), respectively. Then, the mice in groups 2 and 4 were anesthetized and then irradiated with an 808-nm laser at 1 W/$cm^2$ for 5 min after 6 h injection. Subsequently, the body weight and tumor sizes were measured by a balance and caliper every other day for 2 wk. Tumor volume = $4\pi/3 \times$ (tumor length/2) × (tumor width/2)$^2$. Relative tumor volumes were calculated as $V/V_0$; $V_0$ was the initial tumor volume at the start of the treatment. The mice were humanely killed after 2 wk of treatment and all of the tumors were collected from each group.

B16 cells were cultured in RPMI-1640 supplemented with 10% FBS at 37 °C with 5% $CO_2$. A total of $5 \times 10^5$ B16 cells suspended in 100 μL of PBS were injected into the right hind legs of the female BALB/c mice. The subsequent steps were the same as for MDA-MB-231 tumor-bearing mice. The difference is B16 cells grow too fast and the tumor size of the mice in group 1 exceeded 20 mm on the seventh day after treatment, so the body weight and tumor sizes were measured by a balance and caliper every day for 7 d. Finally, the mice were humanely killed after 7 d of treatment and all of the tumors were collected from each group.

**Histology Examination.** The mice were killed, and representative heart, liver, spleen, lung, kidney, and tumor tissues were collected for histology analysis. The tissues were sliced and dehydrated successively and embedded in liquid paraffin and then were sliced to 3–5 mm for H&E staining.

**PTCE.** The PTCE of BPNSs was measured and analyzed by irradiating a 1-cm path-length quartz cuvette containing 1 mL BPNSs dispersion with different concentrations. The NIR laser was generated using an 808-nm, 5-W, fiber-tailed, multimode diode laser (Ningbo Lasever Inc.). The temperature of the irradiated aqueous dispersion was recorded by an infrared thermal imager (FLIR E60).

Following a reported method, when thermal equilibrium within a system is attained much faster than energy exchange with the surroundings, PTCE $\eta$ can be determined by (1)

$$\eta_T = \frac{hA \cdot \Delta T_{max} - Q_s}{I(1 - 10^{-A_{808}})}, \quad \textbf{[S1]}$$

where $\eta$ is the PTCE from incident laser energy to thermal energy, $I$ is incident laser power (in units of milliwatts), $A_{808}$ is the absorbance of the BPNSs at wavelength of 808 nm, $h$ is the heat-transfer coefficient, $A$ is the area of the container, and $\triangle T_{max}$ is the temperature change at the maximum steady-state temperature ($\triangle T_{max} = T_{max} - T_{amb}$, where $T_{max}$ is the maximum system temperature, and $T_{amb}$ is the ambient temperature of the surroundings). $Q_s$ represents heat dissipated from light absorbed by the sample cell itself, and it was measured independently using a sample cell containing pure water without BPNSs. When using borosilicate glass cells containing aqueous samples, $Q_s$ is measured to be $Q_s = (0.54 \cdot I)$ mW. If solvent is not water (e.g., NMP, IPA), $Q_S = I(1 - 10^{-A_{solvent,808}})\eta_{solvent}$, where $A_{solvent,808}$ is the absorbance of the solvent at wavelength of 808 nm, and $\eta_{solvent}$ is the PTCE from incident laser energy to thermal energy; it was measured independently using a sample cell containing that pure solvent.

Once given, the incident laser power $I$ immediately gives $Q_s = (0.54 \cdot I)$ mW. $\triangle T_{max} = T_{max} - T_{amb}$ and $A_{808}$ were easily obtained by measuring. Thus, only the $hA$ remains unknown for calculating $\eta$.

To determine $hA$, a dimensionless driving force temperature $\theta$ is introduced,

$$\theta = \frac{t - T_{amb}}{T_{\max} - T_{amb}}, \quad \textbf{[S2]}$$

where $t$ is the real-time temperature of the BPNSs aqueous dispersion.

Considering the laser irradiation was shut off during the cooling period of the BPNSs aqueous dispersion, a useful relation was deduced as,

$$t = \frac{\sum_i m_i C_{p,i}}{hA} \cdot (-\ln\theta), \quad \textbf{[S3]}$$

where $i$ terms $\sum_i m_i C_{p,i}$ are products of mass and heat capacity of system components (BPNSs aqueous dispersion, sample cell, etc.).

It was clearly shown in Eq. **S4** that $hA$ can be directly derived by applying the linear time data from the cooling stage vs. negative natural logarithm of driving force temperature (the curve "$t$ vs. $-\ln\theta$") and gives

$$\frac{\sum_i m_i C_{p,i}}{hA} = \frac{t}{(-\ln\theta)}. \quad \textbf{[S4]}$$

The left-hand side of Eq. **S4** is the slope of the curve "$t - (-\ln(\theta))$". The curve "$t$ vs. $-\ln\theta$" was immediately obtained by using the dependence of the temperature and time during the cooling period.

Hence, the ratio of $t/(-\ln\theta)$ was obvious to be 205.2 from the slope of the curve $t$ vs. $-\ln\theta$ (Fig. S3*B*). And then the product of $hA$ is deduced to be 0.020467836 mW/°C by using Eq. **S4** and the given data (mwater = 1 g, $C_{p,water}$ = 4.2 J/g).

Finally, the PTCE of BPNSs at 808 nm can be determined to be 38.8% by substituting the value of $hA$ into Eq. **S1**.

**Influence Factors of Drug Release Rate.** Controlled burst release may be advantageous to keep the released drug within its therapeutic window especially as therapeutic drugs often have nonlinear pharmacokinetics. In this section, we demonstrate that the drug release rate and amount can be precisely controlled, depending on the different formulations of BP@Hydrogel.

Specifically, the drug release rate can be modulated by several factors, such as BP and drug concentrations, agarose content, light intensity, and exposure time. On the basis of Fick's second law, the drug release rate can be expressed as a two-order partial differential equation of drug concentration with respect to time and space as

$$\frac{\partial c}{\partial t} = D\frac{\partial^2 c}{\partial r^2}, \quad \textbf{[S5]}$$

where $c$ is the concentration of DOX in solution, $t$ is time, $r$ is distance, and $D$ is diffusion coefficient. The solution formulation of the equation is discussed in detail in the following section. The solution of the equation can be expressed as

$$\mathrm{c}(x,t) = f(x) \cdot e^{-D\beta^2 t} \quad \textbf{[S6]}$$

$$f(x) = \sum_{i=0}^{n} [a_i \cos(i\omega x) + b_i \sin(iwx)], \quad \textbf{[S7]}$$

where $a_i$ and $b_i$ are Fourier transform coefficients. It can be seen from Fig. S5 that the release rates of DOX increase with increasing BP and DOX content and laser power, while they decrease with increasing agarose content. This is reasonable that increased BP content and laser power and decreased agarose content accelerate the softening of the hydrogel, thus enhancing the diffusion coefficient of DOX, while increased DOX concentration increases the concentration gradient. All of the factors contribute comprehensively to the release rate of drugs. The release rate with respect to BP and agarose content is shown in a 3D histogram in Fig. S5*E*. As can be seen in Fig. S5*E*, a high drug release rate can be obtained from high BP content and low agarose content in the case of other conditions unchanged. The drug release rate can be derived from the time derivative of concentration, shown in Fig. S5*F*. The release rate profile tends to stabilize after the initial rapid release, due to the surface adsorbed drug.

**Dynamic of Drug Release.** The drug and water initial distribution is shown in Fig. S6. It is assumed that the drug will diffuse alone the $x$ direction only. On the basis of Fick's second law, the diffusion equation could be expressed as

$$\frac{\partial c}{\partial t} = D\frac{\partial^2 c}{\partial x^2}, \quad \textbf{[S8]}$$

where $c$ is the concentration of DOX in solution, $t$ is time, $x$ is distance, and $D$ is diffusion coefficient. This equation can be solved with the method of separation of variables. Set $c(x,t) = X(x)T(t)$; Eq. **S8** could be expressed as

$$T'X = DX''T,$$

and then

$$\frac{T'}{DT} = \frac{X''}{X} = -\lambda. \quad \textbf{[S9]}$$

Eq. **S9** could be rewritten as

$$\begin{cases} X'' + \lambda X = 0 \\ T' + D\lambda T = 0 \end{cases}. \quad \textbf{[S10]}$$

The eigenfunctions and eigenvalues of Eq. **S10** are different as initial conditions and boundary conditions changed. Set $\lambda = -\beta^2$. It is easy to exclude the solutions which have no physical meaning when $\lambda > 0$ and $\lambda = 0$. When $\lambda < 0$, one solution of Eq. **S8** is

$$c(x,t) = f(x) * e^{-D\beta^2 t}, \quad \textbf{[S11]}$$

where

$$f(x) = \sum_{i=0}^{n} [a_i \cos(i\omega x) + b_i \sin(iwx)]. \quad \textbf{[S12]}$$

$\beta = 2n\pi/ml$, and $a_i$ and $b_i$ are Fourier transform coefficients. We could calculate the concentration anywhere and anytime by Eq. **S11**. While in practice we measure the drug concentration at a fixed position, that means Eq. **S11** is only the function of time $t$. Fig. S7 shows the fitted curve of time and concentration by Eq. **S11**.

1. Roper DK, Ahn W, Hoepfner M (2007) Microscale heat transfer transduced by surface plasmon resonant gold nanoparticles. *J Phys Chem C Nanomater Interface* 111:3636–3641.

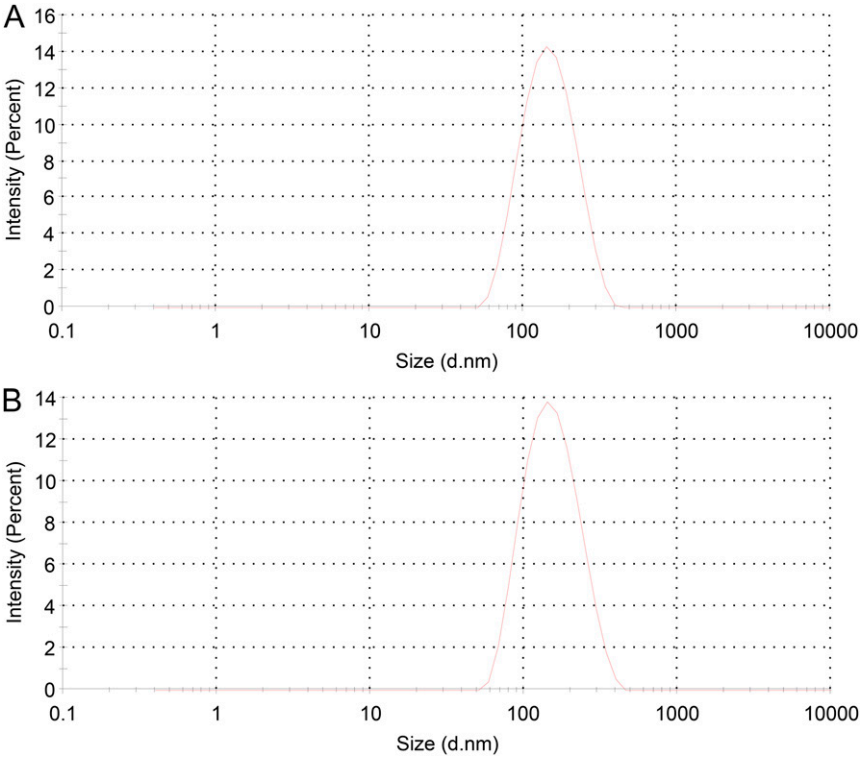


**Fig. S1.** Diameter distribution of (*A*) BPNSs and (*B*) PEGylated BPNSs measured from DLS analysis.

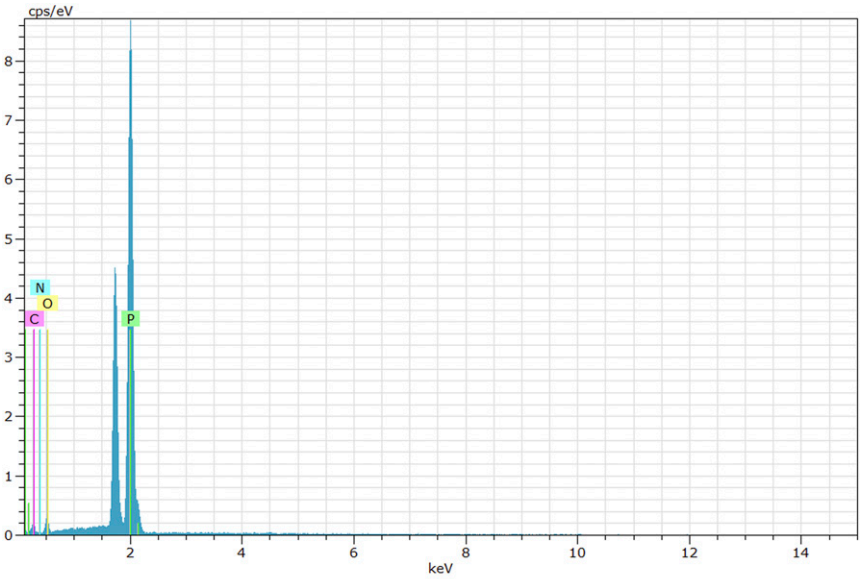


Date: 3/21/2017 3:02:50 PM Pressure: 15.0kV Pulse: 1.85kcps

| El | AN | Series | unn. C [wt.%] | norm. C [wt.%] | Atom. C [at.%] | Error (1 Sigma) [wt.%] |
|---|---|---|---|---|---|---|
| P | 15 | K-series | 48.69 | 67.84 | 47.16 | 1.89 |
| C | 6 | K-series | 14.48 | 20.17 | 36.15 | 3.75 |
| O | 8 | K-series | 6.54 | 9.11 | 12.25 | 1.52 |
| N | 7 | K-series | 2.07 | 2.89 | 4.44 | 1.03 |
| | | Total: | 71.78 | 100.00 | 100.00 | |

**Fig. S2.** EDS of PEGylated BPNSs.

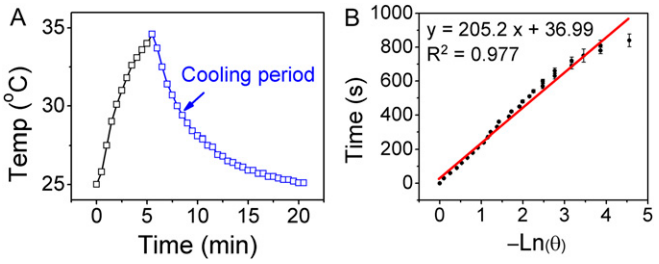


**Fig. S3.** (*A*) Heating and cooling property of deionized water dispersion of BPNSs under irradiation with an 808-nm laser (intensity of 1.0 W·cm$^{-2}$), in which the irradiation lasted for 5 min, and then natural cooling for 15 min. (*B*) Time constant for heat equilibrium system is fitted to be $\tau_s = 205.2s$ by simply applying the data from the cooling period (after 5 min), where the linear time $t$ is directly given by the horizontal ordinate of the cooling period, and the dimensionless driving force temperature $\theta$ can be calculated by $\theta = (t - T_{amb})/(T_{max} - T_{amb})$.

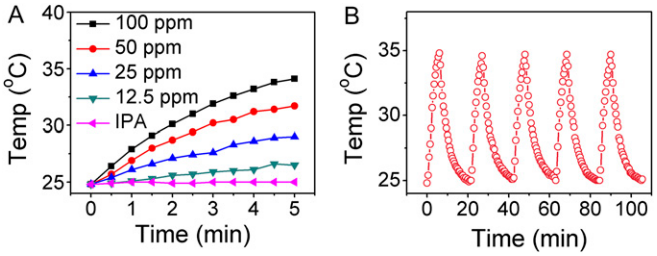


**Fig. S4.** Photothermal property of the as-prepared BPNSs. (*A*) The BPNSs dispersed in IPA at varied concentrations (100 ppm, 50 ppm, 25 ppm, 12.5 ppm) and pure IPA were exposed to an 808-nm diode laser at a density of 1.0 W·cm$^{-2}$. (*B*) Heating of the as-prepared BPNSs suspension dispersed in IPA (100 ppm, 1 mL) with an 808-nm diode laser irradiation (1.0 W·cm$^{-2}$) for five on/off cycles.

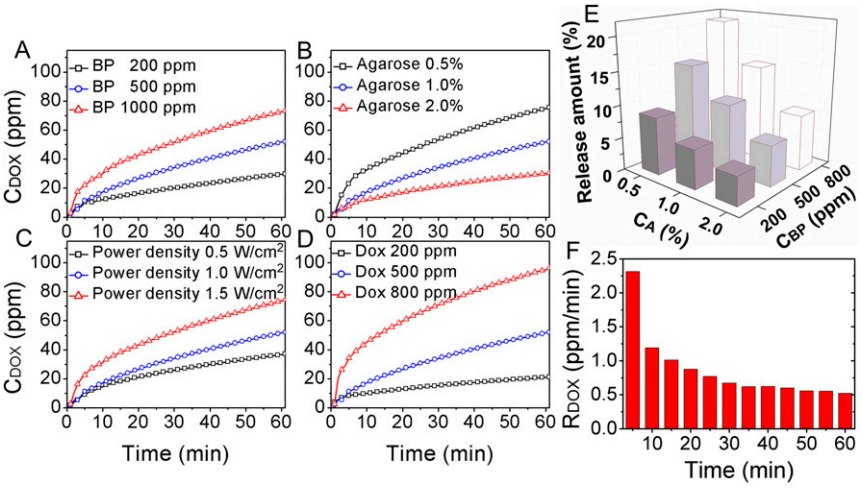


**Fig. S5.** Single-factor experiment of released DOX concentration vs. time evolution. (*A*) BP concentrations ranging from 200 ppm to 500 ppm to 1,000 ppm, agarose content 1%, laser power density 1 W·cm$^{-2}$, DOX concentration 500 ppm. (*B*) Agarose concentrations ranging from 0.5% to 1% to 2%, BP concentration 500 ppm, laser power density 1 W·cm$^{-2}$, DOX concentration 500 ppm. (*C*) The laser power density ranging from 0.5 W·cm$^{-2}$ to 1 W·cm$^{-2}$ to 1.5 W·cm$^{-2}$ with BP concentration 500 ppm, 1% agarose, and DOX concentration 500 ppm. (*D*) The DOX concentration ranging from 200 ppm to 500 ppm to 800 ppm with BP concentration 500 ppm, 1% agarose, and laser power density 1 W·cm$^{-1}$. (*E*) The release amount of DOX vs. BP concentration and agarose content with 1 W·cm$^{-2}$ laser power and preload of 500 ppm DOX at the time of 60 min. (*F*) The DOX release rate ($R_{DOX}$) vs. time evolution with BP 500 ppm, 1% agarose, 1 W·cm$^{-2}$ laser power, and preload of 500 ppm DOX.

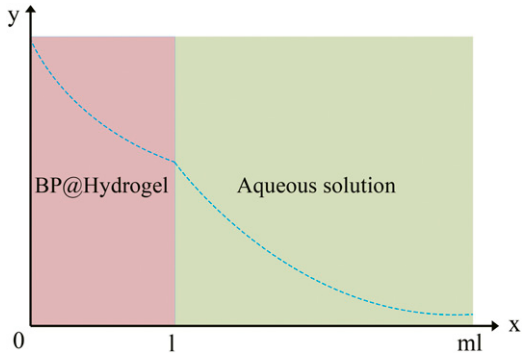


**Fig. S6.** The drug and solution initial distribution. The blue dashed line is the concentration curve at a certain time. The drug deposits at the zone where $0 < x < l$ before the diffusion process begins, while the volume of solution is $m$ times drug, where $m$ is a positive coefficient.

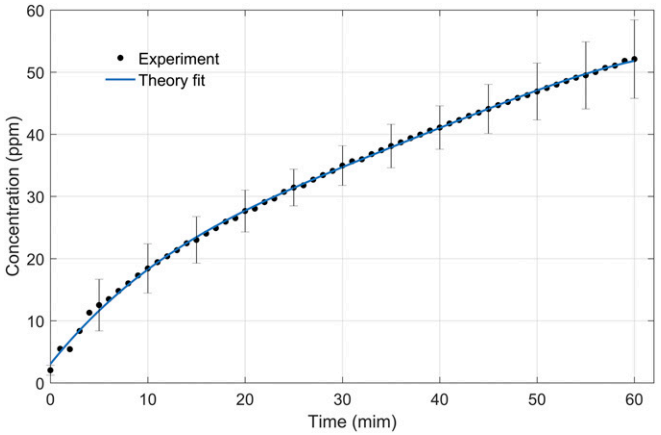


**Fig. S7.** The measured concentration at a fixed position and its fitted curve by Eq. **S11**. The $f(x)$ takes only the first two terms. The fit coefficients are as follows: $a_0$, -1.702e8; $a_1$, 2.269e8; $b_1$, -5.948e6; $a_2$, -5.667e7; $b_2$, 2.972e6; $\omega$, -6.75e-4; and $\sigma$, 0.3772.

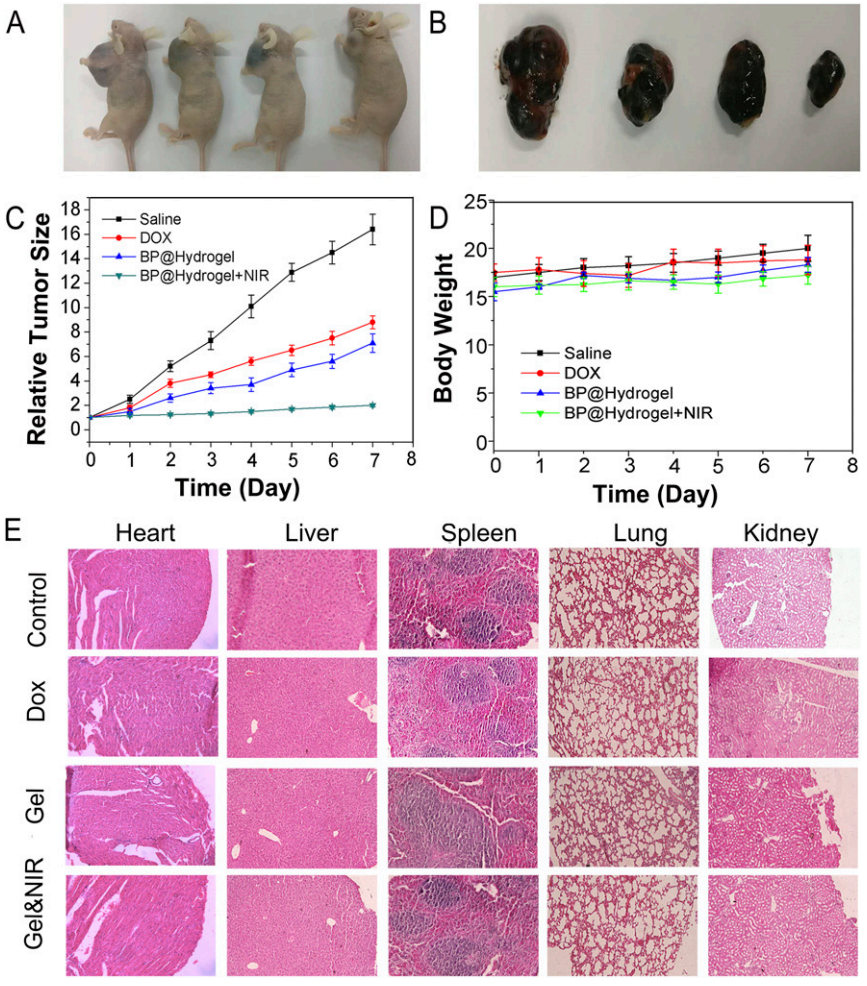


**Fig. S8.** In vivo anticancer effect of BP@Hydrogel drug delivery platform. (*A*) Representative photograph of nude mice bearing s.c. B16 treated with saline, DOX only, BP@Hydrogel only, and BP@Hydrogel with laser irradiation. (*B*) Representative image of the tumors treated with saline, DOX only, BP@Hydrogel only, and BP@Hydrogel with laser irradiation. (*C*) Tumor volumes of nude mice after various treatments. (*D*) Body weight of nude mice taken every other day after various treatments. (*E*) H&E-stained images of major organs from the mice treated with saline, DOX only, BP@Hydrogel only, and BP@Hydrogel with laser irradiation.